

The motion and active deformation of India

J. Paul,¹ R. Bürgmann,² V. K. Gaur,¹ R. Bilham,³ K. M. Larson,⁴ M. B. Ananda,¹ S. Jade,¹ M. Mukal,¹ T. S. Anupama,¹ G. Satyal,⁵ and D. Kumar¹

Abstract. Measurements of surface displacements using GPS constrain the motion and deformation of India and India-Eurasia plate boundary deformation along the Himalaya. The GPS velocities of plate-interior sites constrain the pole of the angular velocity vector of India with respect to Eurasia to lie at $25.6 \pm 1.0^\circ$ N $11.1 \pm 9.0^\circ$ E, approximately 6° west of the NUVEL-1A pole of < 3 Ma plate motion. The angular rotation rate of $0.44 \pm 0.03^\circ$ Myr⁻¹ is 14% slower than the long-term rate of 0.51° Myr⁻¹. Insignificant velocities between plate interior sites indicate that the exposed Indian plate is stable to within $7 \cdot 10^{-9}$ yr⁻¹. The observed contraction vector across the Himalaya (≤ 20 mm/yr) veers from \sim N20°E in the northwest Himalaya to \sim N25°W in east Nepal, consistent with east-west extension of southern Tibet.

Introduction

Since ~ 50 Ma, the Indian subcontinent has been in rapid collision with Eurasia. The width of the zone of convergence ranges from approximately 1500 km in the west, where convergence is about 43 mm/yr, to approximately 3500 km in the east, where approach velocities attain 52 mm/yr [DeMets *et al.*, 1994]. Recent geologic studies of Himalayan frontal thrust faults (HFF) suggest that they absorb as much as 50% of the convergence [Lave and Avouac, 2000].

Freymueller *et al.* [1996], using GPS data collected in Bangalore (IISC) in southern India and at several global GPS sites, found agreement between the current Indian plate motion with that predicted by the < 3 Ma plate motion model, NUVEL-1A [DeMets *et al.*, 1994]. More recent analyses [Chen *et al.*, 2000; Shen *et al.*, 2000], however, suggest that the motion of Bangalore is 5-7 mm/yr slower than NUVEL-1A. GPS data from sites distributed across India permit these estimates to be refined.

The Indian Peninsula is generally considered to be a stable continental shield, however, the occurrence of significant earthquakes in the plate interior indicates that minor deformation occurs within India [Gupta, 1993; Bilham *et al.*, 1998]. While geologic evidence for recent coastal emergence and subsidence remains equivocal [Subrahmanya, 1994], recent tide gauge and leveling data appear to confirm

long wavelength vertical deformation [Bendick and Bilham, 1999]. A GPS survey of triangulation monuments south of 1° N revealed no significant shear strain $> 0.01 \mu$ strain yr⁻¹ in the past 160 years [Paul *et al.*, 1995].

In contrast, convergence across the Himalaya of northern India and Nepal is significant. About 20 mm/yr of India and Eurasia's convergence is accommodated across the Nepal Himalaya [Bilham *et al.*, 1997]. The zone of maximum convergence rates is well north of the surface trace of the HFF system, which accommodates much of the geologic shortening of the last few million years [Lave and Avouac, 2000]. This is consistent with models of elastic strain accumulation north of the rupture zones of past and future great earthquakes, which rupture from the strain accumulation zone southward to the HFF [Bilham *et al.*, 1997]. Earthquake focal mechanisms [Molnar and Lyon-Caen, 1989] suggest that the convergence axis rotates counterclockwise from west to east along the arc to remain in a near arc-perpendicular orientation, consistent with east-west hanging wall extension across southern Tibet [Armijo *et al.*, 1986].

Here we integrate GPS measurements throughout India, including sites in the Garhwal and Kumaon Himalaya, with the data of Larson *et al.* [1999] to (1) determine the motion of the Indian plate, (2) estimate strain within the Indian subcontinent, and (3) constrain the orientation of Himalayan convergence between longitudes 77° - 92° E.

Data Acquisition and Analysis

Site occupations commonly lasted three days, and 20 to 24 hours each day. Data for days when there was physical disturbance to the antenna were excluded from the analysis.

We use the Bernese 4.0 GPS analysis software and precise International GPS Service (IGS) orbits and pole orientation parameters. Station coordinates are computed in the ITRF96 reference frame [Sillard *et al.*, 1998] by applying tight position constraints to the coordinates of IISC, KIT3, and POL2. Average day-to-day repeatabilities of baseline measurements are 3 mm, 8 mm, and 15 mm in the north, east and vertical components, respectively. The Nepal GPS data are analyzed using the GIPSY software developed at the Jet Propulsion Laboratory as described in Larson *et al.* [1999] and are also referenced to ITRF96.

Motion of the Indian Plate

The GPS vectors are defined in a geodetic reference frame (ITRF96), which minimizes misfit with respect to NNR-NUVEL1A for sites outside plate boundary zones. Thus to place the geodetic velocities in an India fixed frame, we subtract the no-net-rotation (NNR) NUVEL-1A [Argus and Gordon, 1991; DeMets *et al.*, 1994] model velocities for India for each site. As noted by previous authors [Chen *et al.*, 2000; Shen *et al.*, 2000], the geodetic data require a slower India plate rate, and we compute a new India-plate mo-

¹CSIR C-MMACS, Bangalore University, India

²Department of Earth and Planetary Science, University of California, Berkeley

³CIRES and Department of Geological Sciences, University of Colorado, Boulder

⁴Department of Aerospace Engineering Sciences, University of Colorado, Boulder

⁵G. B. Pant Institute of Himalayan Environment and Development, Almora, India

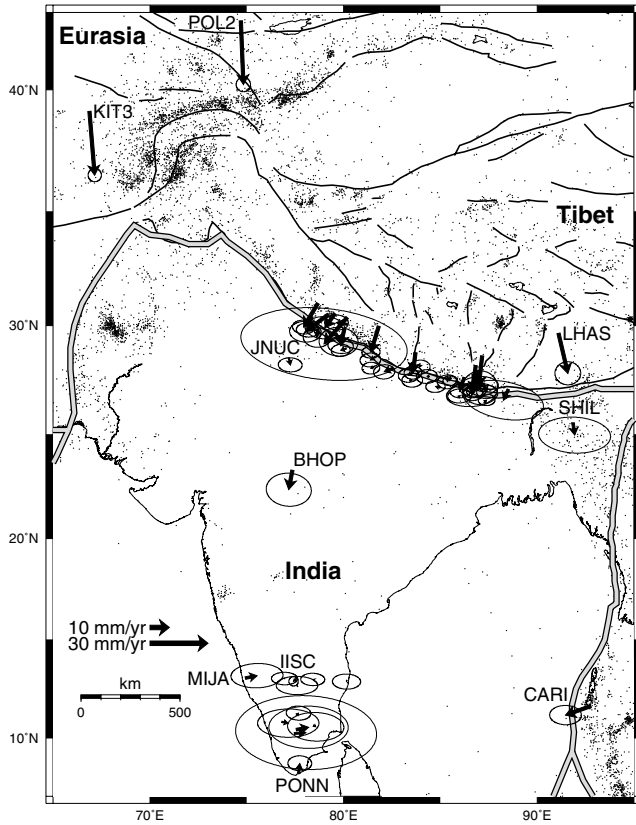


Figure 1. Site velocities determined from 1991-1999 GPS measurements in an Indian reference frame. Bold black lines follow major active fault zones in the collision zone and black dots are 1970-1999 earthquakes. The double lines indicate plate boundaries.

tion angular velocity vector, which minimizes the velocities of sites in the southern Trigon (sites south of 14°N) and at JNUC (Delhi) (Fig. 1). JNUC is on the northernmost exposure of the Archaean crust of India. The geodetically constrained pole of Eurasia-India plate motion thus derived is located at $25.6 \pm 1.0^{\circ}\text{N}$, $11.1 \pm 9.0^{\circ}\text{E}$ with a counterclockwise angular velocity of $0.44 \pm 0.03^{\circ}\text{Myr}^{-1}$ (Fig. 2). This is 6°E and 14% slower than the NUVEL-1A pole-position and angular velocity ($24.5 \pm 1.8^{\circ}\text{N}$, $17.7 \pm 8.8^{\circ}\text{E}$ at $0.51 \pm 0.06^{\circ}\text{Myr}^{-1}$). The India-plate referenced horizontal station velocities are shown in Fig. 1 and Fig. 3.

Deformation of the Indian Plate

The velocities of most sites located on the Indian plate, south of the main frontal thrusts of the Himalaya, are not significantly different from zero (Fig. 1). Data from BHOP 500 km south of the Himalaya are considered unreliable because of an unexplained vertical change of 120 ± 40 mm between 1995 and 1998 and will not be considered further. Only one site in the southern Trigon (PONN) has velocities significantly different from zero at 95% confidence (Fig. 1). We compute uniform horizontal strain tensors from the plate-interior site velocities. With all Trigon sites and JNUC and SHIL included, we find a north-south shortening rate of $6.5 \pm 1.0 \cdot 10^{-9} \text{ yr}^{-1}$ and east-west contraction at $2.6 \pm 4.6 \cdot 10^{-9} \text{ yr}^{-1}$. Excluding PONN, JNUC and SHIL results in 2.1 ± 6.1 and $2.6 \pm 8.4 \cdot 10^{-9} \text{ yr}^{-1}$ strain rates in the north-south and east-west directions, respectively.

Deformation Along the Himalaya

By integrating the Nepal GPS data with the India network data to the west and east, we provide new constraints on convergence along a $\sim 1500\text{-km}$ -long central portion of the Himalayan arc. Southward velocities increase from near zero at the foot of the Himalaya to $15\text{-}22 \text{ mm/yr}$ north of the higher Himalaya (Fig. 3). There is no evidence of significant aseismic accommodation of Himalayan convergence along the portion of the Himalaya currently covered by geodetic observations. The axes of maximum shortening indicated by the GPS data swing counterclockwise from $\sim \text{N}20^{\circ}\text{E}$ at 77°E to $\sim \text{N}25^{\circ}\text{W}$ at 92°E , consistent with arc-normal convergence.

Discussion and Conclusions

Our estimated convergence rate of India relative to Eurasia is 14% slower than that determined from seafloor spreading rates, transform-fault strikes, and focal mechanisms [DeMets *et al.*, 1994]. Holt *et al.* [2000] use a combination of Quaternary fault slip rates and GPS observations to obtain an angular velocity vector at 29.88°N , 7.50°E , with an angular velocity of 0.35 Myr^{-1} (Fig. 2), also indicating a reduced rate. Recent reevaluation of seafloor spreading rates and transform-fault strikes suggests a reduced northward rate of India, by about 25% [Gordon *et al.*, 1999]. Thus, it appears that the difference between active India plate motion and the geologic plate motion model is due to problems in establishing the geologic plate motion circuit (R. Gordon, 2000, pers. commun.), rather than a deceleration of convergence since 3 Ma.

Two recent analyses of the velocity of Bangalore (IISC) relative to Asia also suggest that slower rates prevail than those inferred from NUVEL-1A [Chen *et al.*, 2000; Shen *et al.*, 2000], and slower than those reported by Larson *et al.* [1999]. Subsequent re-analysis of the data used in Larson *et al.* [1999] reveals an error linking the three 1991-97 Bangalore points, whose removal causes all three GPS analyses to agree.

A test of the validity of the NUVEL-1A pole between India and SE-Asia is inconclusive. CARI (Port Blair) on the Andaman Islands is located within the Indo-Asian plate boundary zone (Fig. 1). The unknown degree of seismic cou-

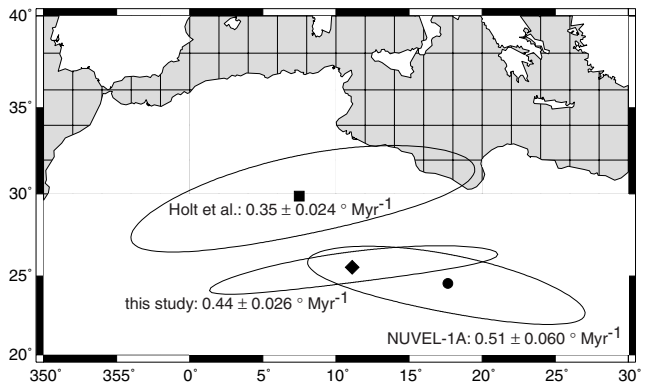


Figure 2. Angular velocity vector poles and rates of Eurasia-India relative motion from sea-floor data (NUVEL-1A), geodetic data (this study), and a combination of regional GPS and geologic fault slip data [Holt *et al.*, 2000].

pling of the east-dipping Indian plate below CARI (Fig. 4) does not permit an independent estimate of the full Andaman velocity. Vector summation diagrams for the India/Andaman/Sunda/Eurasia and India/Andaman/Sunda plate circuits are shown in Fig. 4. Back-arc spreading at 37.2 mm/yr occurs locally at N25°W beneath the Andaman Sea [Curray *et al.*, 1979], and the NUVEL-1A model predicts oblique convergence of the Asian plate at 54.0 mm/yr at N22°E [DeMets *et al.*, 1994]. Sunda motion has recently been reported relative to Eurasia (12-15 mm E) and relative to India (45-52 mm/yr S) [Simons *et al.*, 1999]. The vector diagram of these motions (Fig. 4) indicates that CARI samples approximately 50% of the India/Andaman convergence velocity. If this missing velocity fraction west of Port Blair is ignored, angular closure of the vector diagram is within the errors of measurement. A somewhat better fit is obtained with a 9% reduction in the NUVEL-1A India/Eurasia velocity vector.

Our repeated GPS measurements of sites of the southern Trigon and additional sites in northern India detect no significant strain across India larger than $7 \cdot 10^{-9} \text{ yr}^{-1}$. This result is an order of magnitude lower than our previous estimate of Indian Plate stability based on 160 years of historic triangulation data [Paul *et al.*, 1995]. We elected to not use data from three continuous monitoring stations in the Terai of Nepal in the determination of Indian plate stability, since they monitor a small fraction of the Himalayan convergence field and may include a postseismic deformation signal from the 1934 Bihar/Nepal earthquake. Inclusion of these data would have further reduced the maximum permitted strain rate across India. Geodetic deformation rates are higher than estimates from seismic moment summation of historic ($0.3 - 1 \cdot 10^{-11} \text{ yr}^{-1}$) and instrumental seismic data ($1 - 3 \cdot 10^{-10} \text{ yr}^{-1}$) [Bird and Liu, 2000]. A further decade may be required before we may geodetically determine whether the Indian plate is stable at the level indicated by the rates of seismic moment release.

JNUC and SHIL have southward velocities of $3.7 \pm 1.5 \text{ mm/yr}$ and $6.3 \pm 3.8 \text{ mm/yr}$, respectively. Elastic strain associated with Himalayan convergence decays to negligible southward velocities at these distances [Bilham *et al.*, 1997]. However, it is possible that viscous adjustments near the

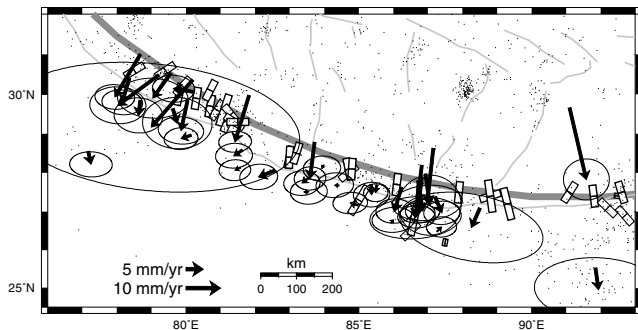


Figure 3. GPS velocities in an Indian reference frame and maximum principal stress axes (open bars from Zoback [1992]) along the Himalayan arc. Convergence and stress axes across the Himalaya rotate counterclockwise by about 45° between 77° and 92° longitude. The bold gray line is a small circle fit to the distribution of moderate Himalayan earthquakes that also coincides with highest topography and other indicators of rapid geologic uplift [Seeber and Gornitz, 1983].

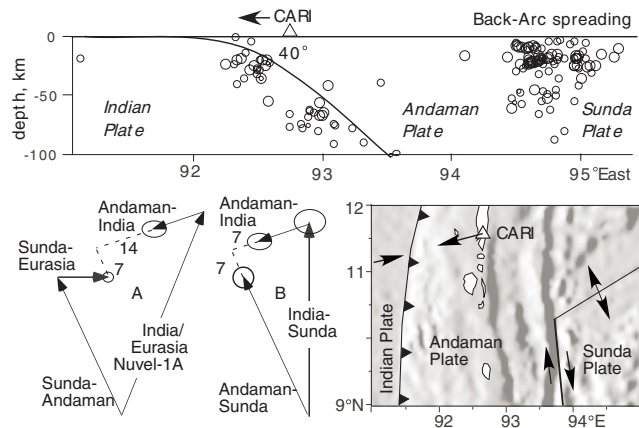


Figure 4. East-west section and map of the Andaman Sea [Engdahl *et al.*, 1998] showing relative motions and vector diagrams for India/Andaman/Sunda/Eurasia and India/Andaman/Sunda plate-circuit closure. Because closure requires approximately double CARI's observed velocity, CARI may be located close to the locking zone of the descending Indian Plate. With this assumption, the remaining misfits in the vector diagrams are not significant at the 1-sigma level, because of the current uncertainties in relative motions in the Andaman Sea.

great 1905 Kangra and 1897 Assam earthquakes north of Delhi and Shillong, respectively, may explain the rates and sense of motion. Alternatively, the observed high rates of seismicity beneath the Shillong Plateau (Fig. 1) may signify that the motion of SHIL is caused by plateau-uplift processes. The southward motion of the Shillong Plateau with respect to India implies that convergence across the Bhutan Himalaya is at least 25% slower than elsewhere in the Himalaya.

Velocity vectors across the Himalaya are approximately arc-normal between longitudes 77° and 92°. The longitude-dependence of these vectors is consistent with the azimuths of maximum principal stress axes (Fig. 3) derived from earthquake focal mechanisms [Zoback, 1992] and east-west extension of southern Tibet at 20 mm/yr [Armijo *et al.*, 1986]. Improved spatial coverage and measurement precision will be required to better resolve the spatial and temporal details of the plate boundary deformation.

Acknowledgments. GPS measurements at Indian sites were carried out under a grant from the Department of Science and Technology of India with considerable logistic support provided by the Directors at the Indian Institute of Astrophysics at Bangalore and the G. B. Pant Institute of Himalayan Environment and Development. GPS Measurements in Nepal are undertaken collaboratively with HMG Survey Department. Special thanks are due to the head of CSIR CMMACS, Bangalore and its computer center administrator Mr. Thangavelu. We thank R. Gordon, W. Holt, R. King, and P. Molnar for valuable discussions and comments on the manuscript. W. Holt, Z.-K. Shen, and R. King kindly provided unpublished results. Research supported by NSF.

References

- Argus, D., and R. Gordon, No-net rotation model of current plate velocities incorporating plate motion model NUVEL-1, *Geophys. Res. Lett.*, 18, 2039-2042, 1991.
- Armijo, R., P. Tapponnier, J.L. Mercier, and H. T.-L., Quaternary extension in southern Tibet; field observations and tectonic implications, *J. Geophys. Res.*, 91, 13,803-13,872, 1986.

- Bendick, R., and R. Bilham, Search for buckling of the southwest Indian coast related to Himalayan collision, *Geol. Soc. Amer. Spec. Pap.*, 328, 313-321, 1999.
- Bilham, R., F. Blume, R. Bendick, and V.K. Gaur, Geodetic constraints on the translation and deformation of India: Implications for future great Himalayan earthquake, *Curr. Sci.*, 74, 213-229, 1998.
- Bilham, R., K. Larson, J. Freymueller, and Project Idylhim, GPS measurements of present-day convergence across the Nepal Himalaya, *Nature*, 386, 61-64, 1997.
- Bird, P., and Z. Liu, Global finite-element model makes a small contribution to intraplate seismic hazard estimation, *Bull. Seism. Soc. Am.*, 89, 1642-1647, 2000.
- Chen, Z., B.C. Burchfiel, Y. Liu, R.W. King, L.H. Royden, W. Tang, E. Wang, J. Zhao, and X. Zhang, GPS measurements from eastern Tibet and their implications for India/Eurasia intercontinental deformation, *J. Geophys. Res.*, 105, 16,215-16,227, 2000.
- Curray, J. R., F. Emmel, D. Moore, R. Raitt, M. Henry, and R. Kieckhefer, Tectonics of the Andaman sea and Burma: *AAPG Mem.*, 29, 189-198, 1979.
- DeMets, C., R.G. Gordon, D.F. Argus, and D. Stein, Effect of recent revisions to the geomagnetic reversal time scale and estimates of current plate motions, *Geophys. Res. Lett.*, 21, 2191-2194, 1994.
- Engdahl, E.R., R.D. Van der Hilst, and R.P. Buland, Global teleseismic earthquake relocation with improved travel times and procedures for depth determination, *Bull. Seism. Soc. Am. Amer.*, 88, 722-743, 1998.
- Freymueller, J., R. Bilham, R. Bürgmann, K.M. Larson, J. Paul, J. S., and V. Gaur, Global Positioning System measurements of Indian plate motion and convergence across the Lesser Himalaya, *Geophys. Res. Lett.*, 23, 3107-3110, 1996.
- Gordon, R.G., D.F. Argus, and M.B. Heflin, Revised estimate of the angular velocity of India relative to Eurasia, *Eos Trans. AGU*, 80, 273, 1999.
- Gupta, H.K., The deadly Latur earthquake, *Science*, 262, 1666-1667, 1993.
- Holt, W.E., N. Chamot-Rooke, X. Le Pichon, and J. Haines, The velocity field in Asia inferred from Quaternary fault slip rates and GPS observations, *J. Geophys. Res.*, 105, 19,185-19,209, 2000.
- Larson, K., R. Bürgmann, R. Bilham, and J.T. Freymueller, Kinematics of the India-Eurasia collision zone from GPS measurements, *J. Geophys. Res.*, 104, 1077-1093, 1999.
- Lave, J., and J.-P. Avouac, Active folding of fluvial terraces across the Siwalik Hills, Himalayas of central Nepal, *J. Geophys. Res.*, 105, 5735-5770, 2000.
- Molnar, P., and H. Lyon-Caen, Fault-plane solutions of earthquakes and active tectonics of the Tibetan plateau and its margins, *Geophys. J. Intl.*, 99, 123-153, 1989.
- Paul, J., et al., Microstrain stability of Peninsular India 1864-1994, *Proc. Indian Acad. Sci. (Earth Planet. Sci.)*, 104, 131-146, 1995.
- Seeber, L., and V. Gornitz, River profiles along the Himalayan arc as indicators of active tectonics, *Tectonophysics*, 92, 335-367, 1983.
- Shen, Z.-K., C. Zhao, A. Yin, Y. Li, D.D. Jackson, P. Fang, and D. Dong, Contemporary crustal deformation in east Asia constrained by Global Positioning System measurements, *J. Geophys. Res.*, 105, 5721-5734, 2000.
- Sillard, P., Z. Altamimi, and C. Boucher, The ITRF96 realization and its associated velocity field, *Geophys. Res. Lett.*, 25, 3223-3226, 1998.
- Simons, W.M.F., B.A.C. Ambrosius, R. Noomen, D. Angermann, P. Wilson, M. Becker, E. Reinhard, A. Walpersdorf, and C. Vigny, Observing plate motions in SE Asia: Geodetic results of the GEODYSSSEA project, *Geophys. Res. Lett.*, 26, 2081-2084, 1999.
- Subrahmanya, K.R., Post-Gondwana tectonics of the Indian Peninsula, *Curr. Sci.*, 67, 527-530, 1994.
- Zoback, M.L., First- and second-order patterns of stress in the lithosphere; the World Stress Map Project, *J. Geophys. Res.*, 97, 11,703-11,728, 1992.
-
- J. Paul, V. Gaur, M Ananda, S. Jade, M. Mukul, T. Anupama, and D. Kumar, CSIR C-MMACS, NAL Campus, Bangalore 560037, India
- R. Bürgmann, Dept. of Earth and Planetary Science, 301 McCone Hall, University of California, Berkeley, Berkeley, CA 94720 (e-mail: burgmann@seismo.berkeley.edu)
- R. Bilham, Dept. of Geological Sciences, University of Colorado, Boulder, CO 80309-216
- K. Larson, Dept. of Aerospace Engineering Sciences, University of Colorado, Boulder, CO 80309-429
- G. Satyal, G. B. Pant Institute of Himalayan Environment and Development, Almora, India

(Received May 30, 2000; revised October 24, 2000; accepted October 31, 2000.)